POLITECNICO DI TORINO
Repository ISTITUZIONALE

A multiphase model of tumour segregation in situ by a heterogeneous extracellular matrix

Original
A multiphase model of tumour segregation in situ by a heterogeneous extracellular matrix / Arduino, A., Preziosi, L.. - In: INTERNATIONAL JOURNAL OF NON-LINEAR MECHANICS. - ISSN 0020-7462. - 75:(2015), pp. 22-30. [10.1016/j.ijnonlinmec.2015.04.007]

Availability:
This version is available at: 11583/2604354 since: 2020-02-18T22:30:57Z

Publisher:
Elsevier

Published
DOI:10.1016/j.ijnonlinmec.2015.04.007

Terms of use:

This article is made available under terms and conditions as specified in the corresponding bibliographic description in the repository

Publisher copyright
Elsevier postprint/Author's Accepted Manuscript

© 2015. This manuscript version is made available under the CC-BY-NC-ND 4.0 license
http://creativecommons.org/licenses/by-nc-nd/4.0/.The final authenticated version is available online at:
http://dx.doi.org/10.1016/j.ijnonlinmec.2015.04.007

(Article begins on next page)

18 November 2026

A Multiphase Model of Tumour Segregation in Situ by a Heterogeneous Extracellular Matrix

A. Arduino, L. Preziosi
Dipartimento di Scienze Matematiche, Politecnico di Torino
Corso Duca degli Abruzzi 24, I-10129, Torino, Italy,
luigi.preziosi@polito.it

April 2, 2015

Abstract

Normal and tumour cells live in a fibrous environment that is often very heterogeneous, even characterized by the presence of basal membranes and regions with high density of collagen fibres that physiologically comparmentalize cells in well defined regions, as for in situ tumours. In case of metastatic tumours these porous structures are instead invaded by cancer cells. The aim of this paper is to propose a multiphase model that is able to describe cell segregation by thick porous structures and to relate the transition rule that determines whether cells will pass or not to microscopic characteristics of the cells, such as the stiffness of their nucleus, their adhesive and traction abilities, the relative dimension of their nucleus with respect to the dimension of the pores of the extra-cellular matrix.

1 Introduction

Recent experiments by Wolf et al. [30] show that cell migration strongly depends on the density of the three-dimensional collagen network they move through and more specifically on the typical size of the pores of the network. They also evaluate the dependence of the cell speed from the pore cross-section, finding a relation that can be considered linear in the range considered (from 5 up to 20 μm^2). In our opinion, the most relevant feature is however the presence of a minimal cross section necessary to allow motion through the three-dimensional extracellular matrix (ECM). Below this threshold, cells try to penetrate with their cytoplasm in the fibre network, but because of the presence of a stiff nucleus, they remain essentially in place (see Fig. 1d bottom). At this point, if the cell is able to express metallo-proteinases (MMPs), these proteins will partially degrade the fibres leading to a local increase in the pore size of the collagen network, forming paths that the cells can use to invade the ECM. On the other hand, cells in which MMP expression is inhibited (like the GM6001 cells in Fig. 1) are not able to penetrate into the network with their entire body, unless the pores are large enough (as in Fig. 1d top). In fact, after 18 hours the border of the multicellular spheroid shown in Fig. 1c has not moved in the rat tail case and has advanced in the bovine case.

Several other experimental papers study the penetration of cells in microchannels [12, 13, 24] interfering with the adhesive and mechanical properties of the cells. On the basis of these experiments and of energy arguments Giverso et al. [8] identified a criterium of penetration involving the comparison of the ratio of adhesion forces exerted by the cells and nucleus stiffness with a given function of the ratio of the microchannel size with respect to the nucleus diameter. In particular, if the size ratio is too restrictive, then the cell cannot penetrate into the micro-channel. However, keeping the same geometrical characteristics, cell clones with higher traction abilities or softer nuclei might be able to penetrate the microchannel. The same dependence was obtained

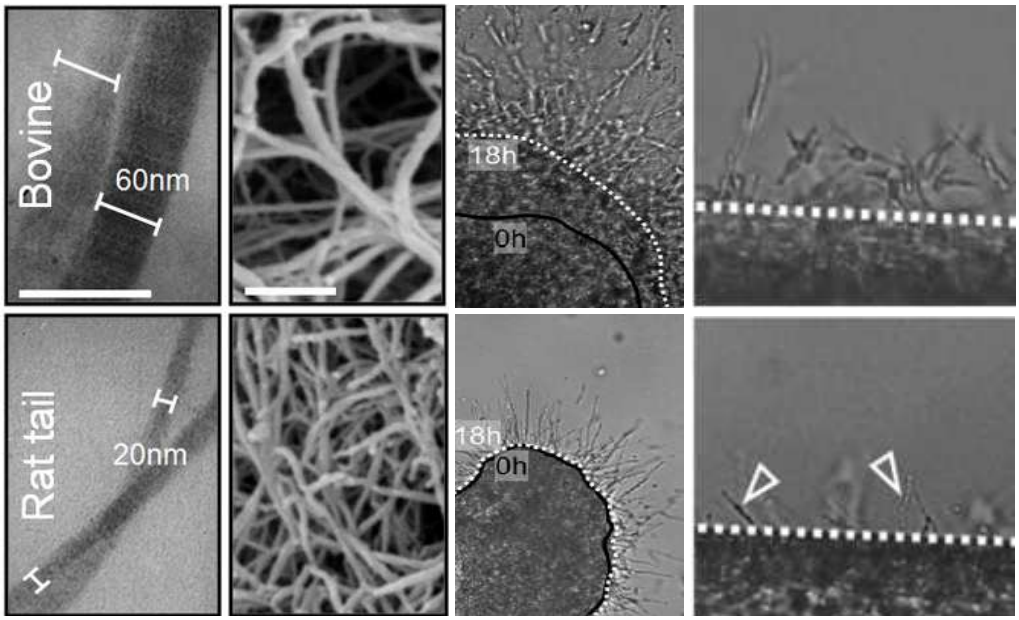


Figure 1: Morphological characteristics of rat tail and bovine collagen fibrils (a; trasmission electron microscopy, bar=0.1μm) and network (b; scanning electron microscopy, bar=1μm). In (c) invasion into rat tail (bottom) and bovine (top) collagen when MMP is inhibited. The rat tail collagen is characterized by a finer mesh and the cell can not penetrate. The arrowheads in the magnified pictures in (d) indicate long cytoplasmic extensions of cells with the nucleus stuck below the collagen. Partially modified from [30] (with permission).

by Scianna et al. [25, 26, 27] who simulated cell migration both over adhesive substrates, and through three-dimensional ECM and microchannels using a cellular Potts model.

Coming back to the experiments by Wolf et al. [30] the above discussion means that the threshold value they find can not be considered constant, but depends on the geometrical and mechanical properties of the cells.

The same mechanism works for multicellular spheroids as well, as shown in Fig. 1c,d and in the supplementary material (Video 3) of [30]. When the spheroid of MMP inhibited cells is embedded in a collagen network which is not too thick, or better with a pore size that is not sterically restrictive, the cells at the boundary of the spheroid tend to invade the gel. On the other hand, if the collagen network is characterized by a pore size that is too small, cells at the boundary tend to protrude into the network but their nucleus remains trapped at the border of the spheroid, so that it can not follow and there is no invasion of the tissue.

Starting from the above experiments in this article we propose a multiphase model that is able to describe cell segregation by thick porous structures. Previous models were not able to include this effect, because they mainly described multicellular spheroids as a fluid (viscous or inviscid) and related the velocity of cells to cell pressure through a sort of Darcy's law with a permeability coefficient that was usually constant or weekly depending on the ECM volume fraction (see the reviews [6, 17, 22, 28, 29]). This implied that any cell pressure would have led to penetration in porous structures, possibly slowed down by the decreased porosity, but segregation was impossible to be achieved.

The model presented here focuses on the term that governs cell motility in the porous ECM. The proposed structure allows to describe situations in which thick regions of ECM can be invaded or not depending on the stiffness of the cell nuclei, on the adhesion and traction ability of cells,

on cell pressure on the ECM, and on the relative dimension of the cell nucleus with respect to the dimension of the pores of the ECM.

The paper then develops as follows. After this introduction and a section presenting the modeling framework, Section 3 contains the main modeling novelties focusing on cell motility. Section 4 discusses the output of the simulation in the case of a single growing population, starting from a control case in which the tumour grows in situ without invading the surrounding tissue. Then several effects leading to tumour invasion are considered such as higher ECM porosity and activation of matrix degrading enzymes. Section 5 generalizes the model to several cell populations, having in mind the goal of describing the growth of a tumour in a normal tissue focusing in particular on the cases in which the tumour population is less sensitive to contact inhibition and have decreased nucleus stiffness, or increased traction ability by the cells.

2 The Basic Mathematical Model

We consider the cell aggregate living in a rigid extracellular matrix (ECM) as a mixture composed of cells and ECM components in the interstitial fluid. Denoting by ϕ_c, ϕ_m, and ϕ_ℓ the volume ratio of cells, ECM, and interstitial fluid and by $\mathbf{v}_c$ and $\mathbf{v}_\ell$ the corresponding velocities, following [5], we can write the following multiphase model

$$\begin{cases} \dfrac{\partial \phi_c}{\partial t} + \nabla \cdot (\phi_c \mathbf{v}_c) = \Gamma_c \,, \\ \nabla \cdot \mathbf{T}_c + \mathbf{m}_c = \mathbf{0} \,, \\ \dfrac{\partial \phi_m}{\partial t} = \Gamma_m \,, \\ \dfrac{\partial \phi_\ell}{\partial t} + \nabla \cdot (\phi_\ell \mathbf{v}_\ell) = \Gamma_\ell \,, \\ \phi_\ell \mathbf{v}_\ell = -\dfrac{\mathbf{K}}{\mu} \nabla P \,, \end{cases} \tag{2.1}$$

where Γ_c, Γ_m and Γ_ℓ are respectively the supplies of cells, ECM and interstitial liquid, $\mathbf{T}_c$ is the stress tensor for the cell population, P is the interstitial pressure, and $\mathbf{m}_c$ is the interaction force between cells and the other constituents. Since our focus will be on growth phenomena in heterogeneous environments, as discussed in [11] the mechanical interactions between the interstitial fluid and the solid constituents (cells and ECM) can be neglected in such slow processes. This leads to the possibility of neglecting the interaction force between cells and interstitial liquid in $\mathbf{m}_c$ and in separating the fluid dynamic problem $(2.1)_{4,5}$ from the remaining equations having solved first the equations related to cell growth and motion.

Regarding the stress tensor for the cellular constituent, following [2, 11, 21, 23] we take

$$\mathbf{T}_c = -\Sigma \mathbf{I} + \mathbf{T}'_c \,, \tag{2.2}$$

with

$$\dot{\mathbf{T}}'_c + \left(\frac{5}{3} \nabla \cdot \mathbf{v}_c - \frac{\Gamma_c}{\phi_c} \right) \mathbf{T}'_c + \frac{\nu}{\eta} \left(\frac{\phi_c}{\phi_n} \right)^{5/3} \mathbf{T}'_c = 2\nu \left(\frac{\phi_c}{\phi_n} \right)^{5/3} \left(\mathbf{D}_c - \frac{1}{3} (\operatorname{tr} \mathbf{D}_c) \, \mathbf{I} \right) \,, \tag{2.3}$$

where $\mathbf{D}_c = \dfrac{\nabla \mathbf{v}_c + (\nabla \mathbf{v}_c)^T}{2}$ and Σ will be specified in the following.

Actually, in some simulations $\mathbf{T}'_c$ is neglected in order to show that even in the simplest (inviscid fluid) situation cell compartimentalization by the ECM can still be achieved.

In principle, one could consider the stress tensor as split in a passive and an active part related to the traction forces that the cell is able to exert by adhering to the ECM and activating the molecular motors (myosins) inside the cytoplasm. However, for the purpose of this article this will not be done here.

In addition, in the following, the action of the production of matrix degrading enzymes from the cells will be also included. This programme is activated by mesenchymal cells in order to cleave the ECM fibres that represent an obstacle to their motion. Hence, this phenomenon will strongly influence cell motility. In fact, by activating metallo-proteinases (MMPs) cells once segregated in certain regions of the tissue are able to invade the surrounding environment. In this case (2.1) will be joined to a reaction-diffusion equation describing the evolution of the concentration c_{MMP} of MMPs

$$\frac{\partial c_{MMP}}{\partial t} = \kappa \nabla^2 c_{MMP} + \gamma_{MMP}\phi_c - \frac{c_{MMP}}{\tau}\,, \tag{2.4}$$

where κ is the diffusion coefficient, γ_{MMP} is the production of MMPs and τ its half life.

The supply of ECM in Eq. $(2.1)_3$ is then modelled assuming that cells are able to produce new peptidic filaments and that MMP molecules degrade the ECM fibres. Denoting by γ_m the deposition rate and δ_m the MMP degradation rate, we can then write

$$\Gamma_m = \gamma_m \phi_c - \delta_m c_{MMP}\phi_m\,. \tag{2.5}$$

3 Cell Motility in ECM

One of the aims of this paper is to describe cell motility in a porous environment and in particular in situations with ECMs thick enough to avoid their penetration, so that growing cell aggregates can not go through them. In order to do that we will refer to the experimental results by Wolf et al. [30] and also to the outcomes of the mathematical models describing the motion of single cells interacting with virtual regular ECMs and microchannels [8, 25, 26, 27] based on other experimental behaviours [12, 13, 24].

As already stated, in growth phenomena it is possible to neglect in $\mathbf{m}_c$ the contribution due to the interaction between cell and interstitial fluid with respect to the one between cells and ECM, so that $\mathbf{m}_c = \mathbf{m}_{cm}$. Focusing on the attachment and detachment processes of the transmembrane proteins deputed to interact with the ECM (mainly integrins) in [21] several constitutive laws have been justified for $\mathbf{m}_{cm}$ starting from microscopic arguments. Here, for sake of simplicity, we take it to be proportional to the relative velocity of cells with respect to the ECM, which at the microscopic level means that integrins constantly renew at the cell membrane independently from the force exerted on the focal adhesion points. Since the ECM is assumed to be rigid, we can then write

$$\nabla \cdot \mathbf{T}_c - \mathbf{M}^{-1}\mathbf{v}_c = \mathbf{0}\,, \tag{3.6}$$

where $\mathbf{M}$, called here motility tensor, takes into account of possible anisotropic situations with strongly aligned ECM fibres in which motion along the fibre bundles is favoured with respect to motion across them, as in the case of invading glioblastoma cells in the brain. However, in the following, we will consider isotropic situations because of lack of experimental data in anisotropic cases and replace $(2.1)_2$ with

$$\mathbf{v}_c = M\nabla \cdot \mathbf{T}_c\,. \tag{3.7}$$

From the experiments described in the introduction [30] it appears that the motility tensor $\mathbf{M}$ in (3.6) can not be considered constant or simply depending on the volume ratio like in Cozeny-Karman rule. There is a threshold pore area A_0 below which there is actually no relative motion of cells with respect to the ECM. Furthermore, it appears that for pore areas sligthly above A_0 the velocity is proportional to $A_m - A_0$ where A_m is the pore area of the ECM, that depends on some volume ratio of ECM. An evaluation of this dependence is given in the Appendix and shown in Fig. 2a. In particular, the figure puts in evidence that for a given ECM volume ratio, different cross sections A_f of the fibre bundles will be related to different pore areas, i.e., at constant ϕ_m the thinner the fibre is, the smaller the pore area is, or in order to have a given pore area smaller fibre bundles require smaller overall volume ratios of the ECM. If $A_m \gg A_f$, as in some physiological cases, then $A_m \approx 9A_f/\phi_m^2$.

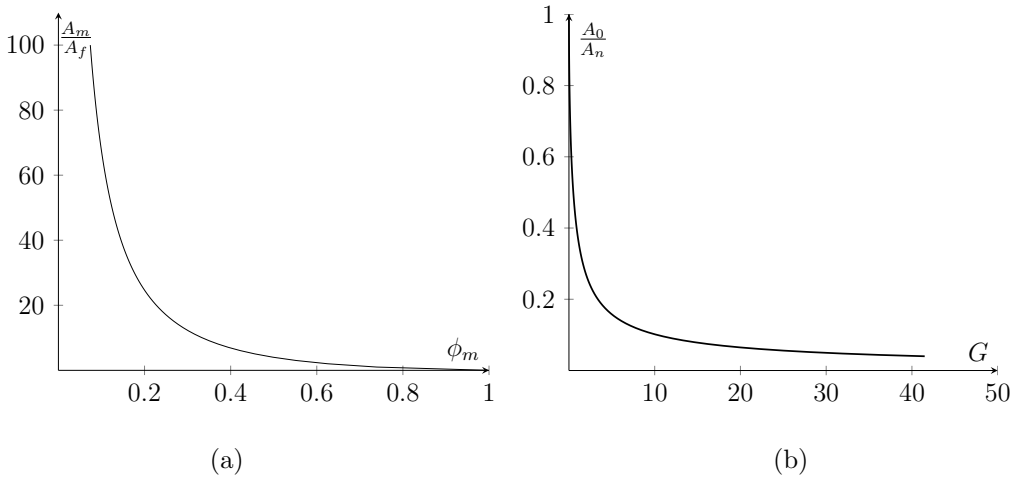


Figure 2: Evaluation of the relationships between pore area and ECM volume ratio (a) and between the scaled threshold pore area and the ratio of stress versus nucleus stiffness given by f^{-1} (see Eq.(3.10) (b).

The motility term M can then be assumed to be given by

$$M = \alpha[A_m(\phi_m) - A_0]_+ \,, \tag{3.8}$$

where $(f)_+ = \frac{f+|f|}{2}$ stands for the positive part of f and α can be evaluated by the experiments in [30].

However, it is known [3, 7, 16, 18, 20, 32] that in both two- and three-dimensional environments cell motion has a bimodal behaviour depending on the ECM structure, porosity, density, adhesion, and stiffness, as also obtained by the simulations of the models described in [25, 26, 27]. This means that there is an optimal ECM density (and therefore pore size) below which traction is not so effective because the number of focal adhesion points that the cell can form is limited, so that they are unable to pull strongly on the ECM and advance. Above this optimal value cells strongly adhere to the ECM and detach with more difficulty from it to move in the ECM. Therefore, a more proper generalization of (3.8) could be

$$M = \alpha \frac{[A_m(\phi_m) - A_0]_+}{\left(1 + \frac{A_m(\phi_m) - A_0}{A_1}\right)^n} \,, \tag{3.9}$$

that reduces to (3.8) for $n = 0$, saturates to a maximum motility αA_1 for $n = 1$ and goes to zero again for large pore areas for $n > 1$. Unfortunately, to our knowledge there are no quantitative experiments that can help in evaluating neither A_1 nor n. However, some hints can be obtained by the simulations given in [25, 26].

Also the threshold value A_0 in general can not be taken constant, because as shown in [8, 25, 26], it depends

- on nucleus stiffness and dimension and
- on cell adhesion and stress.

The former dependence is a measurement of the force or energy needed to deform the shape of the nucleus enough to allow its penetration through pores of a given area. The latter dependence is a measurement of the force that the cell passively experiences due to the pressure of the other cells, or is able to exert by itself attaching and pulling on the ECM fibres in order to pass through the ECM pore. Therefore, in general this last contribution will depend on the density of integrins

expressed at the membrane, on the density of adhesive sites on the ECM, and on the active force due to myosin activation [8].

Denoting by

$$G = \frac{1}{3\mu}|\mathrm{tr}\mathbf{T}_c|\,,$$

where μ is the elastic modulus of the cell nucleus, using the results in [8], we have that the threshold value A_0 can be evaluated by formally inverting the relationship

$$f\left(\frac{A_0}{A_n}\right) = G\,,$$

where

$$f\left(\frac{A_0}{A_n}\right) = \frac{2}{3}\,\frac{2\dfrac{A_0}{A_n} + \dfrac{A_n^2}{A_0^2} - 3}{2\dfrac{A_n}{A_0} - 1 + \sqrt{1 - \dfrac{A_0}{A_n}}}\sqrt{\frac{A_n}{A_0}}\,, \qquad \text{for } A_0 < A_n\,, \tag{3.10}$$

and A_n is the cross section area of the cell nucleus at rest. This gives the relationship

$$A_0 = A_n f^{-1}\left(\frac{1}{3\mu}|\mathrm{tr}\mathbf{T}_c|\right)\,.$$

plotted in Fig. 2b.

For a given pore dimension $A_m(\phi_m)$ it will be also useful to denote by

$$T_m = \mu f\left(\frac{A_m(\phi_m)}{A_n}\right)\,, \tag{3.11}$$

that represents a measure of the traction necessary to pass through pores of area A_m.

4 Growth of an Aggregate in a Heterogeneous Network

In order to test the behaviour of a tumour cell aggregate growing in a heterogeneous environment, we assume that nutrients are abundant everywhere and growth is limited by cell-cell compression only, a phenomenon known as contact inhibition of growth [5]. The growth term is then assumed to be given by

$$\Gamma_c = [\gamma_c \mathcal{H}_\varepsilon(\psi_0 - \psi) - \delta_c]\,\phi_c\,, \tag{4.12}$$

where $\psi := \phi_c + \phi_m$, ψ_0 is the threshold value that models the triggering of contact inhibition, γ_c is the duplication rate of cells, δ_c is the apoptotic rate, $\mathcal{H}_\varepsilon$ is a continuous mollificator of the Heaviside function defined as

$$\mathcal{H}_\varepsilon(\psi) = \begin{cases} 0\,, & \text{if } \psi \le 0; \\ \psi/\varepsilon\,, & \text{if } 0 < \psi \le \varepsilon; \\ 1\,, & \text{if } \psi > \varepsilon. \end{cases}$$

Regarding the constitutive model we take Σ in (2.2) to be given by

$$\Sigma(\psi) = E\frac{1-\phi_n}{1-\psi}(\psi - \phi_n)_+\,, \tag{4.13}$$

where E is analogous to the Young modulus for low compression and ϕ_n is the highest volume ratio below which cells experience no compression.

We can now distinguish between two problems of interest in cell migration: the MMP-independent and the MMP-dependent migration.

To model the first one it is sufficient to set to zero the production rates of MMP, $\gamma_{MMP} = 0$. Assuming that MMP is absent from the domain since the beginning of the simulation, the second

equation in (2.1) and (2.4) become unnecessary, being the distribution of ECM constant in time, though strongly heterogeneous. The solution of this problem would reproduce the behaviour that in [30] has been observed for the so-called GM6001 cells, and thus stress how the newly defined motility catches the interaction between cells and ECM.

It is instructive to observe that if $\mathbf{T}'_c = \mathbf{0}$ the MMP-independent model reduces to the single equation

$$\frac{\partial \phi_c}{\partial t} + \nabla \cdot \left\{ \phi_c \alpha \frac{[A_m(\phi_m) - A_0]_+}{\left(1 + \frac{A_m(\phi_m) - A_0}{A_1}\right)^n} \Sigma'(\psi) \nabla \psi \right\} = \left[\gamma_c \mathcal{H}_\varepsilon(\psi_0 - \psi) - \delta_c\right] \phi_c \,, \tag{4.14}$$

which becomes degenerate when $A_m(\phi_m) = A_0$ and changes type from parabolic, in those time-dependent regions where $A_m(\phi_m) > A_0$ (i.e., where and when cells move), to hyperbolic otherwise. Then the character of the equations is such that the appearance of discontinuities in the volume ratios can not be excluded. For this reason we chose to use a finite volume numerical scheme, that can handle both the parabolic and the hyperbolic nature of the equations and in particular is able to garantee an accurate evaluation of mass balances.

To model the MMP-dependent migration, Eqs.$(2.1)_{1,3}$ must be joined with Eqs.(2.2), (2.3), (2.4), and (3.7). Its solution will simulate situations in which cells confined by too thick ECMs open their own ways by the production of matrix degradation enzymes.

Scaling times with $1/\gamma_c$, lengths with $\sqrt{\alpha A_n E/\gamma_c}$, velocities with $\sqrt{\alpha A_n E \gamma_c}$, stresses with E, and MMP concentration with γ_c/δ_m, it is possible to rewrite the problem in the following dimensionless form

$$\begin{cases} \dfrac{\partial \phi_c}{\partial t^*} + \nabla^* \cdot (\phi_c \mathbf{v}_c^*) = \left[\mathcal{H}_\varepsilon(\psi_0 - \psi) - \delta_c^*\right] \phi_c \,, & \text{in } \Omega^* \\ \dfrac{\partial \phi_m}{\partial t^*} = \gamma_m^* \phi_c - c_{MMP}^* \phi_m \,, & \text{in } \Omega^* \\ \dfrac{\partial c_{MMP}^*}{\partial t^*} = \kappa^* (\nabla^*)^2 c_{MMP}^* + \gamma_{MMP}^* \phi_c - \dfrac{c_{MMP}^*}{\tau^*} \,, & \text{in } \Omega^* \\ \mathbf{v}_c^* \cdot \mathbf{n} = 0 \,, & \text{on } \partial\Omega^* \\ \nabla^* c_{MMP}^* \cdot \mathbf{n} = 0 \,, & \text{on } \partial\Omega^* \end{cases} \tag{4.15}$$

with

$$\mathbf{v}_c^* = \left(A^*(\phi_m) - A_0^*(\psi)\right)_+ (-\nabla^* \Sigma^* + \nabla^* \cdot \mathbf{T}_\mathbf{c}^*) \,,$$

and

$$\dot{\mathbf{T}}_c'^* + \left(\frac{5}{3} \nabla^* \cdot \mathbf{v}_c^* - \frac{\Gamma_c^*}{\phi_c}\right) \mathbf{T}_c'^* + \frac{1}{\eta^*} \left(\frac{\phi_c}{\phi_n}\right)^{5/3} \mathbf{T}_c'^* = 2\nu^* \left(\frac{\phi_c}{\phi_n}\right)^{5/3} \left(\mathbf{D}_c^* - \frac{1}{3} (\operatorname{tr} \mathbf{D}_c^*) \mathbf{I}\right) \,,$$

where the stars denote non-dimensional quantities and where

$$A^*(\phi_m) := \frac{1}{A_n} A(\phi_m) \,, \qquad A_0^*(\psi) := \frac{1}{A_n} A_0(\psi) = f^{-1}\left(E^* \Sigma *\right) \,,$$

Notice that in absence of quantitative experimental data on the behaviour of the motility for large pore areas, we set $n = 0$ in (3.9) for the simulations to follow. The problem then depends on the following dimensionless parameters

$$\delta_c^* = \frac{\delta_c}{\gamma_c} \,, \quad \eta^* = \frac{\eta \gamma_c}{\nu} \,, \quad \nu^* = \frac{\nu}{E} \,, \qquad E^* = \frac{E}{\mu} \,,$$

$$\kappa^* = \frac{\kappa}{\alpha A_n E} \,, \quad \gamma_m^* = \frac{\gamma_m}{\gamma_c} \,, \quad \gamma_{MMP}^* = \frac{\delta_m \gamma_{MMP}}{\gamma_c^2} \,, \quad \tau^* = \gamma_c \tau \,,$$

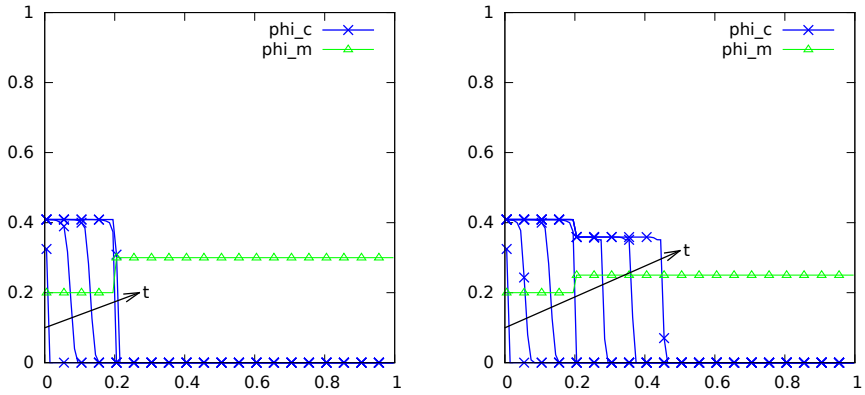


Figure 3: Evolution of the volume ratio of MMP-inhibited tumour cells for $\delta_c^* = 1/8$, $\eta^* = 10$, $\nu^* = 1$, $E^* = 25$, $A_f^* = 0.16$. On the left, $\phi_m^+ = 0.3$ and $t = 4.000, 7.649, 9.598, 11.936, 17.404$. On the right, $\phi_m^+ = 0.25$ and $t = 4.000, 7.128, 9.598, 11.936, 15.719, 21.391, 27.715$. When reaching the region with a denser ECM, on the left tumour cells will stop because the network is too tight, while on the right they are able to pass through the dense ECM region.

in addition to the already dimensionless parameters ψ_0, ϕ_n, and ε, that were set to $\psi_0 = \phi_n = 0.6$, and $\varepsilon = 0.01$ in all simulations and to $A_f^* = A_f/A_n$ that is needed to define A_0^*, as described in the appendix.

As a test case we consider our domain as divided in two parts by a region, denoted by Ω_m, characterized by a higher density of ECM. Specifically,

$$\phi_m(\mathbf{x}, t=0) = \begin{cases} \phi_m^+\,, & \text{if } \mathbf{x} \in \Omega_m \\ \\ 0.2\,, & \text{otherwise} \end{cases} .$$

In the MMP-inhibited case shown in Fig. 3 (left), tumour cells start growing but when they reach the region $\Omega_m = [0.2, 1]$ with a denser ECM with $\phi_m^+ = 0.3$ they are not able to penetrate in and remain segregated. In Fig. 3 (right) the ECM is not thick enough and therefore the cells are able to pass through the network and invade Ω_m. Specifically, the decrease of the ECM density ϕ_m^+ from 0.3 to 0.25 is such that upon reaching this region the value of A_0 is now below A_m there, so that the overcompression of the tumour cells by itself is enough to allow motility in the region Ω_m.

In presence of matrix degrading enzymes a different mechanism leads to cell invasion as shown in Figure 4. In fact, tumour cells are now able to remodel the ECM by the secretion of new fibres and by the expression of MMPs. This causes a digestion of the excessive part of the ECM close to the border of the growing aggregate. Hence, though slowed down, the tumoural invasion is successful. Notice that cells do not penetrate the thick ECM region, but rather decrease the ECM density, i.e., increase the pore areas of the ECM channels to penetrate the thick zone Ω_m.

5 A Two-population Generalization

In view of the application of the model to tumours growing in a normal tissue, we will generalize the above model to two cellular sub-populations. The first one, denoted by $i = 1$, is representative of normal cells, the second one, denoted by $i = 2$, is instead representative of abnormal cancerous cells, that by mutation have lost contact inhibition of growth. This means that

$$\Gamma_c^i = \left[\gamma_c^i \mathcal{H}_\varepsilon(\psi_0^i - \psi) - \delta_c^i\right] \phi_c^i\,, \qquad i = 1, 2\,, \tag{5.16}$$

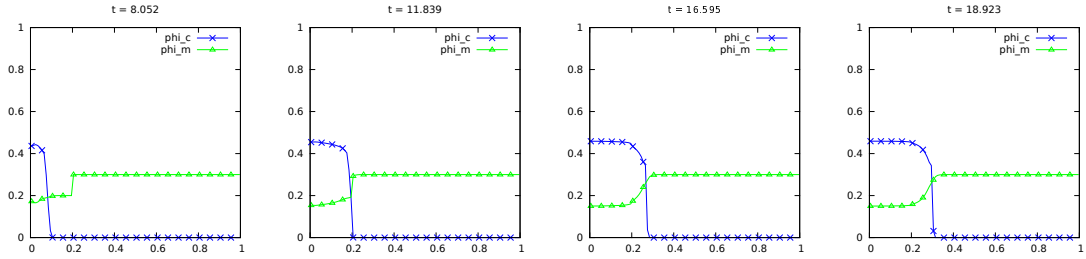


Figure 4: Evolution of one dimensional system when cells are able to express MMPs at $t = 8.052, 11.839, 16.595, 18.923$. In the simulation $\gamma_m^* = 0.15$, $\kappa^* = 6 \times 10^{-5}$, $\gamma_{MMP}^* = 50$, $\tau^* = 0.02$ and $\phi_m^+ = 0.3$, other parameter being as in Fig. 3.

in particular with $\psi_0^2 > \psi_0^1$ leading to different contact inhibition responses. In addition, tumour cells might have different mechanical properties, e.g., softer nuclei.

Regarding the stress tensor, for sake of simplicity we assume here that the cell aggregate behaves like an elastic fluid $\mathbf{T}_c^i = -\Sigma(\psi)\mathbf{I}$, in order to show that segregation also occurs for such a simple (compressible invisid fluid) constitutive equation.

In this case, neglecting the interaction between the two cell populations, because cell cytoplasm can deform much more easily than ECM fibres, Eq.(4.14) is replaced by the two equations

$$\frac{\partial \phi_c^i}{\partial t} + \nabla \cdot \left\{ \phi_c^i \alpha \frac{[A_m(\phi_m) - A_0^i]_+}{\left(1 + \frac{A_m(\phi_m) - A_0^i}{A_1}\right)^n} \Sigma'(\psi) \nabla \psi \right\} = \left[\gamma_c^i \mathcal{H}_\varepsilon(\psi_0^i - \psi^i) - \delta_c^i\right] \phi_c^i \,, \qquad i = 1, 2 \,, \quad (5.17)$$

where $\psi = \phi_c^1 + \phi_c^2 + \phi_m$ is the overall volume ratio of cells and ECM. We notice that the numerical integration of Eq.(5.17) is not straightforward at all, not only for the presence of the cross diffusion term represented by the gradient of the sum of the two volume ratios but also because of the fact that the region in which the two equations might degenerate and change type from parabolic to hyperbolic (identified by the sign of $A_m(\phi_m) - A_0^i$) is usually different for the two sub-populations and will depend on the evolution of their volume ratios.

Regarding MMP remodelling, it is assumed that only tumour cells are able to secrete matrix degrading enzymes and to produce ECM. So, in Eqs.(2.4, 2.5) ϕ_c is replaced by ϕ_c^2.

Considering tumour cells as a genetic mutation of normal cells we will consider most of the parameters of the model to be identical for the two populations. As already stated, the two populations differ for the level of sensitivity to compression ($\psi_0^1 = 0.6$ and $\psi_0^2 = 0.7$ in (5.17) in all simulations). Then we will focus on the different behaviour determined by a change of density of ECM in the thick regions $\Omega_m = \{\mathbf{x} : 0.45 < y < 0.55\}$, of cell stiffness, and on the expression of MMPs. In this case the regions below and above Ω_m are filled with normal cells in equilibrium that cannot penetrate Ω_m because the corresponding pore area A_m is smaller than A_0^1 at ϕ_n.

The following simulations will reproduce what happens when a little portion of a sane tissue transforms into cancerous cells because of loosing contact inhibition of growth. Considering first the MMP-inhibited case, we insert some tumour cells on the bottom-left corner, that because of reduced contact inhibition tend to spread all over the place. In fact, the misperception of the compression state induces an abnormal proliferation of tumour cells that can sustain a relatively more compressed state, compressing in turn the normal cells nearby. Feeling overcompressed, the normal tissue then does not proliferate and only apoptosis occurs, so that the normal cells gradually die and are replaced by the growing tumour.

The starting (control) simulation shown in Figure 5 describes how under suitable conditions the presence of a tumour clone might be segregated by Ω_m representing a sort of growth of an in situ (ductal) carcinoma. In fact, the higher value of stress achieved by the tumor cells is still not sufficient for overcoming the segregation condition. When tumour cell reach the region Ω_m they

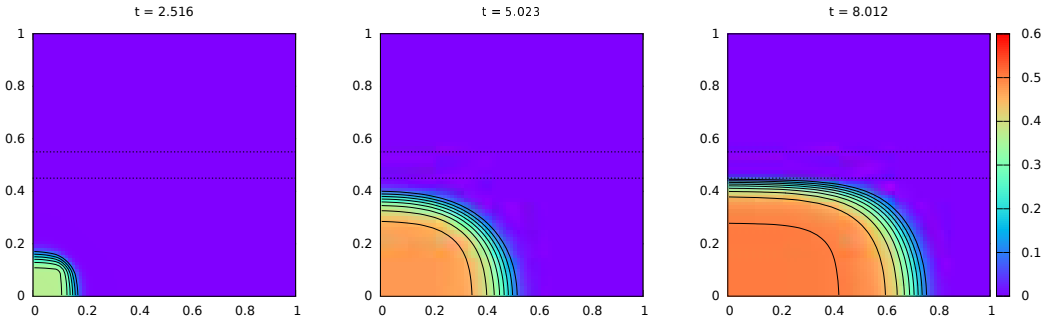


Figure 5: Evolution of the volume ratio of MMP-inhibited tumour cells for $\delta_c^* = 1/8$, $E^* = 25$, $A_f^* = 0.16$ and $\phi_m^+ = 0.3$. When reaching the region with a denser ECM, tumour cells will stop and continue to grow along it.

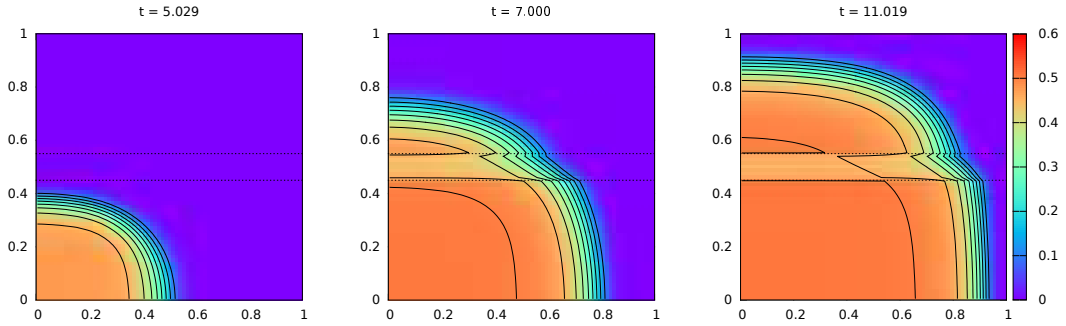


Figure 6: Evolution of the volume ratio of MMP-inhibited tumour cells for $\phi_m^+ = 0.25$, other parameter being as in Fig. 5. The evolution before reaching the region with a denser ECM, is similar to the previous figure. In this case, however, tumour cells are not stopped, and, though slowed down, are able to pass through the denser region.

are not able to pass through it and growth will continue along the region with a denser ECM to fill progressively the region below Ω_m. Eventually, the tumour clone will completely replace the normal tissue reaching a segregated equilibrium with tumour cells below Ω_m, normal cells above Ω_m and no cells in Ω_m.

The following simulations show how a change in a single parameter is able to change completely the situation and induce invasion through the region Ω_m. Before reaching Ω_m the simulation is qualitatively similar to that shown in Fig. 5. Specifically, in Figure 6 the decrease of the ECM density ϕ_m^+ in the region Ω_m from 0.3 to 0.25 is such that upon reaching this region the value of A_0^2 is now below A_m there, so that the overcompression of the tumour cells by itself is able to cause a transition through the region Ω_m of tumour cells still keeping normal cells segregated below Ω_m. Cells are actually slowed down by the higher density of ECM but can efficaciously reach out the upper region even in absence of activation of MMPs.

A qualitatively similar behaviour is observed when other parameters influencing the segregation rule are changed. We will only present here the case in which the nucleus of tumour cells is softer than that of sane cells as it is known experimentally, *i.e.*, $\mu^2 < \mu^1$. This is a very interesting situation from the biomedical point of view because it represents a differentiation of purely mechanical origin that is able to induce a cell invasion dynamics as shown in Figure 7. The simulation is represented in one dimension, in order to give a more clear view of the results about the evolution of the volume ratio of both the populations and of the overall volume ratio ψ. Upon

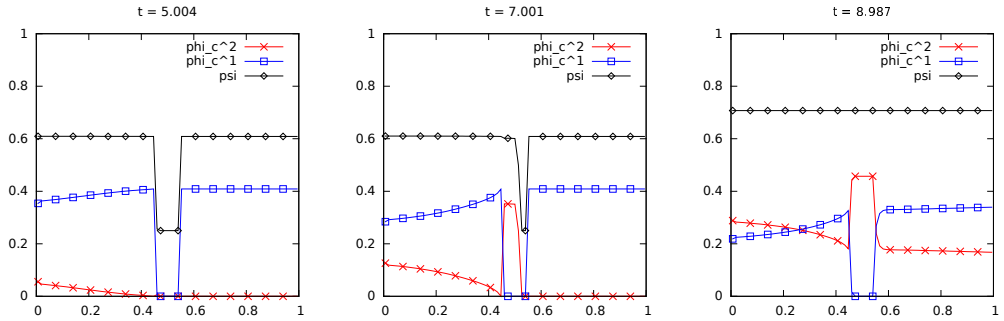


Figure 7: Evolution of one dimensional MMP-inhibited system for $E^{1*} = 25$, $E^{2*} = 37.5$ and $\phi_m^+ = 0.3$, other parameter being as in Fig. 5. Tumour cells thanks to their softer nucleus are able to invade the region Ω_m that is too dense for the stiffer nucleus of sane cells, also in the compressed configuration.

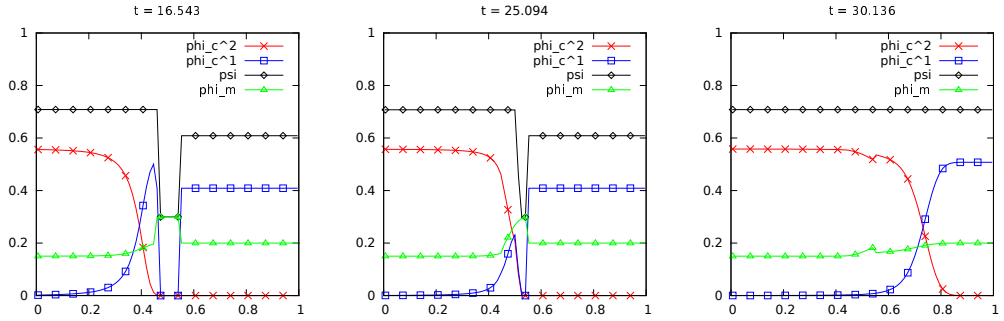


Figure 8: Evolution of one dimensional system when MMP production is activated for $\kappa^* = 6 \times 10^{-5}$, $\gamma^*_{MMP} = 50$, and $\tau^* = 0.02$, other parameter being as in Fig. 5. Tumour cells growth compressing the sane cells against the denser region Ω_m, until they reach it and there remodel the ECM opening their own way.

reaching Ω_m not only the tumour cells are able to penetrate it but they also completely populate it so that the overall volume ratio ψ is eventually constant everywhere.

A different phenomenon occurs when MMPs are expressed. Recovering the configuration of the control simulation we further assume that only the tumour clone is now able to remodel the ECM by the secretion of new fibres and of MMPs. This causes the cleavage of the excessive part of the ECM that is then restored after the passage of the tumour cells. Therefore, though slowed down, tumoural invasion is successful through a smoothing of the thickest ECM. In Figure 8 a one dimensional simulation shows the evolution of the volume ratios of the cell populations and of the ECM.

The last simulation in Figure 9 gives the evolution of an MMP-inhibited tumour in a heterogeneous tissue where it can be appreciated how neither normal nor tumor cells are able to penetrate the most dense regions of a very heterogeneous tissue. The ECM is distinguished into three regions: the low density one with $\phi_m = 0.2$ (from below, the first, third, fifth, and seventh stripe), the high density one with $\phi_m = \phi^+_{m,1}$ and the medium density one with $\phi_m = \phi^+_{m,2}$. All cells are able to move in low density regions, and tumour cells also in medium density ones; no cell is instead able to penetrate the highest density regions. So, in conclusion, tumour cells are able to find their way through higher density areas.

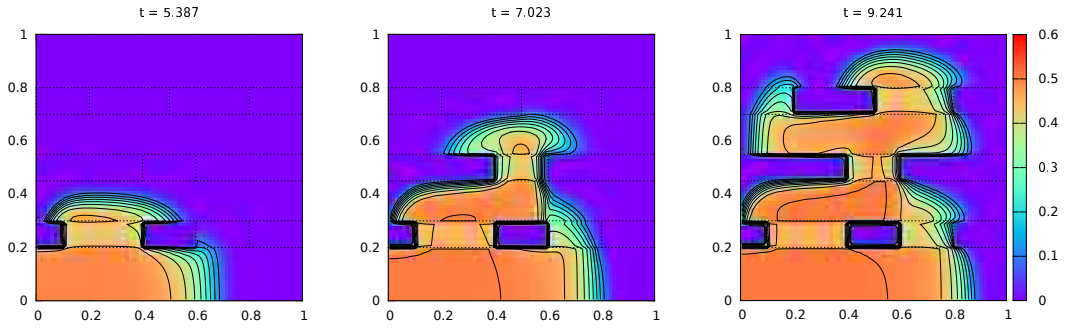


Figure 9: Evolution of the volume ratio of MMP-inhibited tumour cells for $\phi^+_{m,1} = 0.3$, $\phi^+_{m,2} = 0.25$, other parameter being as in Fig. 5. The tumour growths in the heterogeneous tissue avoiding denser regions.

6 Discussion

In this paper we have deduced a model that is able to describe situations in which cell aggregates and growing tumours can be compartimentalized by porous structures with a sufficiently low pore dimension. The model is characterized by a presence of a threshold that was put in evidence by several experiments and that depends on several microscopic characteristics of the cells. The most relevant one is the ratio of the dimension of the pore area of the ECM with respect to that of the nucleus, which is the stiffest part of the cell, because it determines how much the nucleus must compress in order to squeeze in the ECM pores. Of course, the amount of energy and the work to be done depends on the nucleus stiffness and on the ability of the cells to pull on the ECM or on the pressure the growing tissue is exerting on the compartimentalizing ECM. Simulations show that changing one of the parameters related to the above characteristics might determine whether the surrounding normal tissue will be invaded or not by the tumour. The case of MMP expession is also modelled giving rise to a disruption of the thickest regions of ECM and to the invasion of the normal tissue beyond it.

The model deduced is very challenging for those who want to study its analytical properties because even in the case of a single population the equations may change type, being hyperbolic in those region when there is no motion (but there might be possibly growth) and degenerate parabolic in the regions where cells move with respect to the ECM. In the presence of more cell population the mathematical model is also characterized by cross diffusion.

In addition, the problem is usually characterized by the presence of free boundaries, which suggest the use of level set methods from the numerical point of view. For instance, if there is an interface dividing a cell-free region from a region where cells are duplicating, this interface will not move if the stress is below T_m which according to (3.11) depends, for instance, on the stiffness of the nucleus and on the ratio of the pore area of the ECM and the section of the nucleus. If the tissue grows so that at the surface the threshold is overcome, then the interface will move together with the cells and the problem becomes degenerate parabolic with an interface condition on the stress.

The model can be improved in several aspects. From the mechanical point of view one could consider more complex constitutive laws regarding the behaviour of cells, or the interaction of the cellular population with the ECM, or the active forces that mesenchymal cells exert on the ECM. In addition one could drop the hypothesis of a rigid ECM.

Also from the physiological point of view, it would be interesting to modify the model to treat the case of thin basal membranes or going more in details in the remodelling of the ECM. Finally, it would be very interesting to achieve a closer comparison with the migration modes triggered by different ECM confinements as those reported in [14, 15].

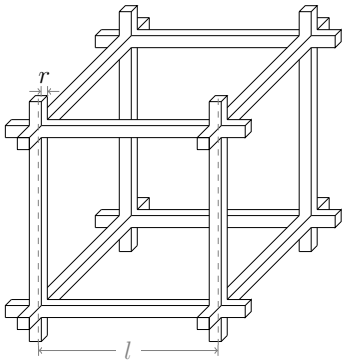


Figure 10: Schematization of a regular structure of the ECM.

Appendix

In the study of problems where ECM remodelling plays an important role, for example in the case of MMP-dependent motion of cells, it is important to evaluate how the pore area A_m of the ECM, parameter necessary in the definition of the motility of cells through the matrix, is related to the volume ratio ϕ_m of the ECM, known from the solution of the relative mass balance equation.

A relation between these two quantities is reacheable assuming that the ECM is constituted by peptide fibres locally disposed as a uniform orthogonal cartesian crystal lattice, as in Figure 10. Assuming for sake of simplicity that geometrically the fibres have a square cross section with thickness $2r$, and that the side of each crystal cell is l, it is possible to state that in a single crystal cell $V_{\text{tot}} = l^3$ and $V_{\text{ECM}} = 12lr^2 - 8r^3$, and thus recover the relation between l and ϕ_m,

$$\phi_m = \frac{V_{\text{ECM}}}{V_{\text{tot}}} = 4(3x^2 - 4x^3)\,, \tag{6.18}$$

where $x = r/l$.

On the other hand, the following obvious relation between the pore area A_m and the crystal cell's side holds

$$A_m = (l - 2r)^2 = r^2 \left(\frac{1}{x} - 2\right)^2 . \tag{6.19}$$

From the definition of the crystal cell arises the physical constrains $r, l > 0$ and $2r < l$, thus the non-dimensional quantity x must obey to the inequalities $0 < x < \frac{1}{2}$. It may be interesting to notice the extreme behaviours: when x tends to zero, *i.e.* $l \gg r$, the porous area grows indefinitely; viceversa when x tends to $\frac{1}{2}$, *i.e.* $l \sim 2r$, the porous area decreases toward zero. For any $\phi_m \in [0, 1]$, the number x can be easily computed as the only root of the polynomial (6.18) that belongs to $[0, \frac{1}{2}]$.

To obtain a relation between ϕ_m and A_m, Eq. (6.19) can be inverted to give

$$x = \frac{1}{\dfrac{\sqrt{A_m}}{r} + 2}\,,$$

and substituted back in (6.18) to obtain

$$\phi_m = \frac{3\sqrt{\dfrac{A_m}{A_f}} + 1}{\left(\sqrt{\dfrac{A_m}{A_f}} + 1\right)^3}\,,$$

where we have used the fact that in this case $A_f = 4r^2$. Notice that for $A_f \ll A_m$, as in some physiological cases, $\phi_m \approx 3\sqrt{\frac{A_f}{A_m}}$.

The proposed relation is qualitatively in agreement with experimental results. Indeed, in [30] it is observed that matrices obtained by collagen fibrils extracted by bovine dermis are constituted of bigger pores than matrices of the same density (*i.e.*, volume ratio) obtained by fibres extracted by rat tail. The first collagens are characterized by 60 nm thick fibrils, while the latter by 20 nm thick fibrils (see Fig. 1a). According to the proportionality between A_m and A_f in (6.19), these measurements are sufficient to justify the above mentioned observation.

However, it need be mentioned that in physiological tissue several fibrils run aligned and are organised in fibre bundles with a thickness that can reach up to a couple of micrometers which is almast equal to the radius of a cell nucleus.

Similar results can be obtained replacing square section fibres with cylinders. However, in this case at maximum packing $l = 2r$ the volume ratio ϕ_m does not reach 1 because of voids in the center of the cubic lattice, while $A_m \to 0$.

Assuming that cylinders do not cross but are orthogonally tangent to each other, then Eq. (6.18) is replaced by $\phi_m = 3\pi x^2$ ($\phi_m = 12x^2$ in the case of square section fibres) with x being limited by $x \leq 1/4$ for geometric reasons. In this case getting close to close packing gives some problems in uniquely identifying the pore area. As before, when $x \to 1/4$, $\phi_m \to 3\pi/16 < 1$ ($\phi_m \to 3/4$ in the case of square sections).

However, when $A_f \ll A_m$, as in most cases, all evaluations collapse to the same estimate $\phi_m \approx 3\sqrt{\frac{A_f}{A_m}}$ mentioned above.

Acknowledgments

The authors wish to thank K. Wolf (Radboud University Medical Centre) for sharing with us the data and helping in understanding them and the Italian Institute for High Mathematics for partially funding this research.

References

[1] D. Ambrosi, L. Preziosi. On the closure of mass balance models for tumour growth, *Math. Mod. Meth. Appl. Sci.* **12**, 737–754 (2002).

[2] D. Ambrosi, L. Preziosi. Cell adhesion mechanisms and stress relaxation in the mechanics of tumours. *Biomech. Model. Mechanobiol.* **8**, 397–413 (2009).

[3] B.T. Burgess, J.L. Myles, R.B. Dickinson, Quantitative analysis of adhesion-mediated cell migration in three-dimensional gels of RGD-grafted collagen, *Ann. Biomed. Eng.* **28**, 110–118 (2003).

[4] H.M. Byrne, L. Preziosi, Modeling solid tumour growth using the theory of mixtures, *Math. Med. Biol.* **20**, 341–366 (2004).

[5] M.A.J. Chaplain, L. Graziano, L. Preziosi. Mathematical modelling of the loss of tissue compression responsiveness and its role in solid tumour development. Math. Med. Bio. 23: 197-229 (2006).

[6] V. Cristini, J. Lowengrub, Eds., **Multiscale Modeling of Cancer: An Integrated Experimental and Mathematical Modeling Approach**. Cambridge University Press, 2010.

[7] P.A. DiMilla, J.A. Stone, J.A. Quinn, S.M. Albelda, D.A. Lauffenburger, Maximal migration of human smooth-muscle cells on fibronectin and type-IV collagen occurs at an intermediate attachment strength, *J. Cell. Biol.* **122**, 729–737 (1993).

[8] C. Giverso, A. Grillo, L. Preziosi, Influence of nuclear deformability on cell entry into cylindrical structures, *Biomech. Model. Mechanobiol.*, **13**, 481-502 (2014).

[9] C. Giverso, L. Preziosi, Modelling the compression and reorganization of cell aggregates, *Math. Med. Biol.* **29**, 181-204 (2012).

[10] C. Giverso, L. Preziosi, Behaviour of cell aggregates under force-controlled compression, *Int. J. Non-Linear Mech.* **56**, 50–55 (2013).

[11] C. Giverso, M. Scianna, A. Grillo, Growing avascular tumours as elasto-plastic bodies by the theory of evolving natural configurations, *Mech. Res. Comm.*, submitted.

[12] J. Guck, F. Lautenschläger, S. Paschke, M. Beil. Critical review: Cellular mechanobiology and amoeboid migration. *Integr. Biol.* **2**, 575–583 (2010).

Y. Komai, T. Ushiki, The three-dimensional organization of collagen fibrils in the human cornea and sclera *Inv. Opht. Visual Sci.* **32** 2244–2258(1991).

[13] F. Lautenschläger, S. Paschke, S. Schinkinger, A. Bruel, M. Beil, J. Guck. The regulatory role of cell mechanics for migration of differentiating myeloid cells *Proc. Natl. Acad. Sci. USA* **106**, 15696 – 15701 (2009).

[14] A. Haeger, M. Krause, K. Wolf, P. Friedl, Cell jamming: collective invasion of mesenchymal tumor cells imposed by tissue confinement. *Biochim Biophys Acta* **1840**, 2386–2395 (2014).

[15] O. Ilina, G.J. Bakker, A. Vasaturo, R.M. Hofmann, P. Friedl, Two-photon laser-generated microtracks in 3D collagen lattices: principles of MMP-dependent and -independent collective cancer cell invasion, *Phys Biol.* **8**, 015010 (2011). Erratum in:*Phys Biol.* **8**, 029501 (2011).

[16] M.P. Lutolf, J.L. Lauer-Fields, H.G. Schmoekel, A.T. Metters, F.E. Weber, G.B. Fields, J.A. Hubbell, Synthetic matrix metalloproteinase-sensitive hydrogels for the conduction of tissue regeneration: Engineering cell-invasion characteristics, *Proc. Natl. Acad. Sci. USA* **100**, 5413–5418 (2003).

[17] J.S. Lowengrub, H.B. Frieboes, F. Jin, Y.L. Chuang, X. Li, P. Macklin, V. Cristini, Nonlinear modelling of cancer: Bridging the gap between cells and tumours, *Nonlinearity* **23**, R1–R9, (2010).

[18] K. Maaser, K. Wolf, C.E. Klein, B. Niggemann, K.S. Zänker, E.B. Bröcker, P. Friedl, Functional hierarchy of simultaneously expressed adhesion receptors: Integrin $\alpha 2\beta 1$ but not CD44 mediates MV3 melanoma cell migration and matrix reorganization within three-dimensional hyaluronan-containing collagen matrices, *Mol. Biol. Cell.* **10**, 3067–3079 (1999).

[19] bundle1 M. Misfeld, H.H. Sievers, Heart valve macro- and micro-structure, *Phil. Trans. R. Soc. B* **362**, 1421—1436 (2007).

[20] S.P. Palecek, J.C. Loftus, M.H. Ginsberg, D.A. Lauffenburger, A.F. Horwitz, Integrin-ligand binding properties govern cell migration speed through cell-substratum adhesiveness, *Nature* **385**, 537–540 (1997).

[21] L. Preziosi, D. Ambrosi, C. Verdier, An elasto-visco-plastic model of cell aggregates, *J. Theor. Biol.* **262**, 35–47 (2010).

[22] L. Preziosi, A. Tosin, Multiphase and multiscale trends in cancer modelling, *Math. Model. Nat. Phenom.* **4** 1–11, (2009).

[23] L. Preziosi, G. Vitale, A multiphase model of tumour and tissue growth including cell adhesion and plastic re-organisation, *Math. Models Methods Appl. Sci.*, **21**, 1901–1932 (2011).

[24] C. G. Rolli, T. Seufferlein, R. Kemkemer and J. P. Spatz, *Impact of tumor cell cytoskeleton organization on invasiveness and migration: a microchannel-based approach*, PLoS ONE, **5**, e8726 (2010).

[25] M. Scianna, L. Preziosi, K. Wolf, A Cellular Potts Model simulating cell migration on and in matrix environments, *Math. Biosci. Engng.* **10**, 235–261 (2013).

[26] M. Scianna, L. Preziosi, Modeling the influence of nucleus elasticity on cell invasion in fiber networks and microchannels, *J. Theor. Biol.*, **317**, 394-406 (2013).

[27] M. Scianna, L. Preziosi, A cellular Potts model for the MMP-dependent and -independent cancer cell migration in matrix microtracks of different dimensions, *Comp. Mech.* **53**, 485–497 (2014).

[28] P. Tracqui, Biophysical models of tumour growth, *Rep. Prog. Phys.* **72**, 056701, (2009).

[29] C. Verdier, J. Etienen, A. Duperray, L. Preziosi, Review. Rheological properties of biological materials, *Compt. Rend. Physics* **10**, 790–811 (2009).

[30] K. Wolf, M. te Lindert, M. Krause, S. Alexander, J. te Riet, A.L. Willis, R.M. Hoffman, C.G. Figdor, S.J. Weiss, P. Friedl, Physical limits of cell migration: Control by ECM space and nuclear deformation and tuning by proteolysis and traction force, *J. Cell Biol.* **201**, 1069–1084 (2013).

[31] K. Wolf, Y.I. Wu, Y. Liu, J. Geiger, E. Tam, C. Overall, M.S. Stack, P. Friedl, Multi-step pericellular proteolysis controls the transition from individual to collective cancer cell invasion. *Nat. Cell. Biol.* **9**, 893–904 (2007).

[32] M.H. Zaman, L.M. Trapani, A.L. Sieminski, D. Mackellar, H. Gong, R.D. Kamm, A. Wells, D.A. Lauffenburger, P. Matsudaira, Migration of tumor cells in 3D matrices is governed by matrix stiffness along with cell-matrix adhesion and proteolysis, *Proc. Natl. Acad. Sci. USA* **103**, 10889–10894 (2006).